PNAS
www.pnas.org

Supporting Information for

Ferroptosis as a novel target for protection against cardiomyopathy

Xuexian Fang, Hao Wang, Dan Han, Enjun Xie, Xiang Yang, Jiayu Wei, Shanshan Gu, Feng Gao, Nali Zhu, Xiangju Yin, Qi Cheng, Pan Zhang, Wei Dai, Jinghai Chen, Fuquan Yang, Huang-Tian Yang, Andreas Linkermann[1], Wei Gu[1], Junxia Min[1] and Fudi Wang[1]

[1] To whom correspondence may be addressed. Email: fwang@zju.edu.cn, junxiamin@zju.edu.cn, or wg8@cumc.columbia.edu, or andreas.linkermann@ukdd.de.

This PDF file includes:

www.pnas.org/cgi/doi/10.1073/pnas.1821022116

SI Materials and Methods

Mice

Ripk3$^{-/-}$ mice were originally generated by Dr. Xiaodong Wang (National Institute of Biological Sciences, Beijing)(1), and provided by Drs. Yan Zhang and Rui-Ping Xiao (Peking University)(2). *Mlkl*$^{-/-}$ and *Fadd*$^{-/-}$*Mlkl*$^{-/-}$ mice were provided by Dr. Haibing Zhang (Shanghai Institutes for Biological Sciences)(3). *Nrf2*$^{-/-}$ mice were originally generated by Dr. Masayuki Yamamoto (Tohoku University)(4), and provided by Dr. Jingbo Pi (China Medical University). Wild-type C75BL/6 mice (8-10 weeks old) were obtained from SLRC Laboratory Animal Co., Ltd. Only male animals were used in this study due to a significant gender difference with respect to DOX-induced cardiotoxicity(5). Unless stated otherwise, the mice were fed a standard rodent laboratory diet containing 232 mg iron/kg (Research Diets). Both the low-iron (0.9 mg iron/kg) and high-iron (8.3 g carbonyl-iron/kg) diets were egg white-based 174 AIN-76A-diets (Research Diets).

Zebrafish

Transgenic zebrafish *Tg(cmlc2:GFP)* with green fluorescent protein (GFP) specifically expressed in the myocardial cells were provided by Dr. Bo Zhang (Peking University) and used following instructions as previously described(6). Adult male and female zebrafish were maintained under a 14 hour light/10 hour dark cycle at 28.5℃ with recirculating deionized water, and embryos were staged by standard methods(7). All zebrafish experimental protocols were approved by the Animal Care and Use Committee of Zhejiang University. Zebrafish embryos of 2 days post-fertilization (dpf) were distributed into a 12-well microplate (20 fish per well), and were treated with DOX (65 μM) in the presence or absence of Fer-1 (1 μM) or DXZ (200 μM) for another 48 h.

In vivo drug treatment

For acute experiments, 8-week-old male mice received a single i.p. injection of DOX (Cat#S1208, Selleck Chemicals, 10 mg/kg or 20 mg/kg body weight dissolved in sterile saline) or saline; 24 or 96 h after injection, the animals were anesthetized for testing, and blood samples and saline-perfused organs were collected for analysis. Hemin (Cat#51280, Sigma, 2.5 mg/ml) was dissolved in 10% ammonium hydrochloride and then diluted in 0.15 M sodium chloride, and i.p. injected into mice (10 ml/g body weight) to induce *Hmox1* expression. Where indicated, mice were i.p. injected with ZnPP (Cat#282820, Sigma, 10 mg/kg dissolved in 10% DMSO and then diluted in sterile saline;) 24 and 2 h before DOX treatment. Where indicated, mice were given a daily i.p. injection of Fer-1 (Cat#S7243, Selleck Chemicals, 1 mg/kg), Nec-1 (Cat#S8037, Selleck Chemicals, 1 mg/kg), 3-MA (Cat#S2767, Selleck Chemicals, 20 mg/kg), emricasan (Cat#S7775, Selleck Chemicals, 2.5 mg/kg), or vehicle one day before DOX treatment. Each inhibitor was dissolved in DMSO, and then diluted in sterile saline. TEMPO (5 mg/kg dissolved in saline; Cat#176141, Sigma) or MitoTEMPO (Cat#SML0737, Sigma, 5 mg/kg dissolved in sterile saline) was i.p. injected to scavenge lipid peroxide. To assess the effect of KN-93 on

DOX-induced mortality, daily KN-93 i.p. injection (Cat#T2697, TargetMol, 10 μmol/kg dissolved in sterile saline;) or an equivalent volume of saline was started on the day of DOX treatment (20 mg/kg).

I/R myocardial injury and infarct size measurement

Adult male C57BL/6 mice (10-12 weeks old) were anesthetized with pentobarbital (70 mg/kg, i.p) and placed in a supine position on a heating pad (37 ℃). Following sedation, mice were intubated and ventilated on a SAR-830 volume-cycled small animal ventilator (CWE Inc.). A left thoractomy was performed around the third intercostal space, and the left anterior descending (LAD) coronary artery was reversibly ligated using sterile 7-0 silk suture with a slipknot. Proper ligation was confirmed by visual observation of the left ventricle wall turning pale. After 30 min of regional ischemia, the heart was allowed to reperfuse, leading to loss of the discoloration of the myocardium distal to the ligation. Fer-1 (1 mg/kg) or DXZ (50 mg/kg) was administered by intraperitoneal injection 24 and 2 hours before surgery. Sham-operated animals underwent the same procedure without ligation of the LAD coronary artery.

To measure the infarct size, the animals were reanesthetized after a 24-hour reperfusion period. The LAD was tightly re-occluded, and Evans blue dye (5%; E2129, Sigma) was injected through external iliac vein. After being excised and rinsed in phosphate buffer saline, the heart was frozen at -20 ℃ for 20 min and cut transversely into slices (4-5 slices/heart). There slices were incubated for 20 min with 1.5% 2,3,5-triphenyltetra-zolium chloride (TTC; Sigma) solution to visualize the unstained infarcted region. The infarct size (IF), area at risk (AAR), and nonischemic left ventricle were assessed with were analyzed by ImageJ (NIH).

Measurement of serum non-heme iron, serum total bilirubin and hematological parameters

Blood samples were collected and centrifuged for 10 min at 3000 rpm to obtain serum. Serum non-heme iron and total iron-binding capacity (TIBC) were measured using the Iron/TIBC Reagent Set (I7506-60; Pointe Scientific) in accordance with the manufacturer's instructions(8). Total serum bilirubin levels were measured by a cobas 6000 chemistry analyzer (Roche). Hematological parameters were measured using ADVIA 2120i hematology analyzer (Siemens) at the Center for Drug Safety Evaluation and Research, Zhejiang University.

Measurement of tissue non-heme iron

Tissue non-heme iron levels were measured using the chromogen method(9). Tissues were weighed and digested in NHI acid (10% trichloroacetic acid in 3 M HCl) for 48 h at 65-70 ℃. Equal volumes of sample or iron standard (500 μg/dl) were incubated for 10 min at room temperature in 200 μl BAT buffer (0.2% thioglycolic acid and 0.02% disodium-4,7-diphenyl-1,10-phenanthroline disulfonate in 50% saturated NaAc solution). Samples were read at 535 nm, and unknowns were calculated using a standard curve. The results are presented in micrograms of iron per gram of wet tissue

weight.

Heme measurement

Serum and tissue heme levels were measured using the QuantiChrom Heme Assay Kit (DIHM-250, BioAssay Systems) in accordance with the manufacturer's instructions(10). In brief, heme was measured in 10 μl of serum or tissue homogenate by measuring the absorption at 400 nm and comparing the value with a standard curve of known heme concentrations.

ICP-MS detection

Determination of total elemental iron in the heart was carried out by inductively coupled plasma mass spectrometry (ICP-MS) as described previously(11). An Agilent 7700x ICP-MS equipped with an Agilent ASX 520 auto-sampler was used to measure the element.

Heme oxygenase activity

Heme oxygenase activity was using the paired enzyme assay in which heme is converted to biliverdin by heme oxygenase and then to bilirubin by biliverdin reductase in the presence of an NADPH-generating system. in brief, 100 μl of heart tissue homogenate (containing approximately 1 mg of protein) was added to a reaction mixture containing 1 mM NADPH in 100 mM potassium phosphate buffer (pH 7.4) supplemented with 1 mM EDTA, 25 μM hemin, and 1 nM bilirubin reductase. The reaction mixture was incubated under constant agitation for 1 hour at 37 ℃ in the dark. After chloroform extraction, the samples were centrifuged, and the organic phase was collected for subsequent spectrophotometric determination of bilirubin concentration. Finally, the samples were scanned using an EON microplate spectrophotometer (BioTek) to calculate the difference in absorption between 450 nm and 520 nm. Heme oxygenase activity is expressed as the formation of bilirubin (in pmol) per hour per milligram of protein.

Measurement of MDA content

Serum and cardiac malondialdehyde (MDA) levels were measured using a kit (Cat#S0131, Beyotime) in accordance with the manufacturer's instructions.

Cell culture and *in vitro* treatment

H9c2 rat cardiomyocytes were obtained from the Cell Bank of Shanghai Institutes for Biological Sciences, Chinese Academy of Sciences, and cultured in Dulbecco's modified Eagle's medium (Gibco) supplemented with 10% heat-inactivated fetal bovine serum (Gibco) and 1× penicillin-streptomycin (Gibco). The cells were incubated at 37 ℃ in a humidified atmosphere containing 5% CO_2 and 95% air. DOX was applied to the cells the indicated concentrations, and inhibitors (Fer-1, DXZ, and zVAD) were applied at the indicated concentrations.

Cell viability assay

Cell viability assay was performed using the CellTiter-Glo® Luminescent Cell Viability Assay kit (Cat#G7572, Promega). Cells were seeded at 5×10^3 cells per well in a 96-well opaque plate. After the indicated treatment, the luminescent signal was measured using GloMax-Multi Detection System (Promega) in accordance with the manufacturer's instructions. Based on the recorded luminescence, the percentage of cell viability was then calculated accordingly.

Flow cytometry-based lipid peroxidation assay

Cells were seeded at 10^6 cells per well in a 6-well plate and treated as indicated. After 12 hours of treatment, the cells were incubated in 2 μM C11-BODIPY$^{581/591}$ (Invitrogen) for 20 minutes at 37℃ in the dark, then analyzed using a Cytomics FC 500 flow cytometer (Beckman Coulter). BODIPY emission was measured using the FL-1 channel. Data were collected from a minimum of 10,000 cells.

Caspase 3/7 assay

Caspase 3/7 activity was measured using the Caspase 3/7-Glo assay (Cat#G8091, Promega) and the GloMax-Multi Detection System (Promega) in accordance with the manufacturer's instructions.

Histology

Hearts were fixed overnight in 4% paraformaldehyde (pH 7.4), embedded in paraffin, and serially sectioned at 5-μm thickness. The sections were stained with Hematoxylin and Eosin (H&E) for routine histological examination with a light microscope. To measure collagen deposits, select sections were stained with Sirius red. For each mouse, three adjacent sections were quantified using ImageJ software (National Institutes of Health).

Immunohistochemistry and iron staining

Serial sections were deparaffinized, blocked with phosphate-buffered saline (PBS) containing 5% (v/v) normal goal serum and 1% (w/v) BSA), and then incubated overnight with rabbit anti-mouse-ferroportin (1:200) or anti-4 hydroxynonenal (ab46545; 1:200; Abcam) at 4℃ under humidified conditions, followed by incubation for 1 hour with anti-rabbit secondary antibody (1:500 dilution, Proteintech) at room temperature. Non-heme iron staining was measured using a standard Perls' Prussian Blue stain as previously described (12). Photomicrographs were obtained using an Eclipse E400 microscope (Nikon).

Quantitative real-time PCR

Total RNA was isolated from tissues or cells using Trizol (Pufei), and RNA concentration and purity were measured using a spectrophotometry. RNA was reverse-transcribed using the PrimeScript RT reagent Kit (Takara) in accordance with the manufacturer's instructions. Quantitative PCR was performed using a CFX96 Real-Time System (Bio-Rad) and SYBR Green Supermix (Bio-Rad) in accordance with the manufacturer's instructions. The fold difference in gene expression was

calculated using the $2^{-\triangle\triangle Ct}$ method and is presented relative to *Gapdh* mRNA. All reactions were performed in triplicate, and specificity was monitored using melting curve analysis. See **Table S3** for the PCR primers used.

RNA sequencing and data analysis

Whole-genome gene expression analysis was performed using the heart tissues from DOX- and saline-treated mice (n=3 per group) at 24h. The total RNA was extracted using Trizol (Pufei), and cDNA samples were sequenced using a sequencing system (HiSeq3000; Illumina). The reference *Mus musculus* genome and gene information were downloaded from the National Center for Biotechnology Information database. Raw reads were filtered to produce high-quality clean data. All the subsequent analyses were performed with the clean data. All the differentially expressed genes were used for heat map analysis and KEGG ontology enrichment analyses. For KEGG enrichment analysis, a *P*-value<0.05 was used as the threshold to determine significant enrichment of the gene sets.

Western blot analysis

Nuclear proteins were extracted from fresh heart tissue using the NE-PER Nuclear and Cytoplasmic Extraction Reagents (Cat#78833; Thermo Scientific). Total proteins were extracted from the tissues by homogenizing in RIPA buffer containing protease inhibitors. The homogenate was cleared by centrifugation at 4℃ for 30 min at 12,000 rpm, and the supernatant (containing the protein fraction) was collected. Protein concentration in the supernatant was measured using the BCA Protein Assay Kit (Beyotime). A total of 20 mg protein per sample was resolved in a 10-12% SDS-PAGE and transferred to a nitrocellulose membrane. The membranes were blocked with 5% BSA in Tris-buffered saline containing 0.2% Tween-20, then incubated with primary antibodies at 4℃ overnight. The following antibodies were used: anti-Hmox1 (1:1000; Cat#ab13243, Abcam), anti-Hmox2 (1:500; Cat#sc-17786, Santa Cruz Biotechnology); anti-Nrf2 (1:1000; Cat#ab137550, Abcam); anti-Histone H3 (1:1000; Cat#9715, Cell Signaling Technology); anti-Total OxPhos (1:500; Cat#ab110413, Abcam); anti-Porin (1:1000; Cat#66345, Proteintech) and anti-Gapdh (1:10000; Cat#MB001, Bioworld). The membranes were then washed and probed with the appropriate horseradish peroxidase–conjugated secondary antibodies (1:4000; Proteintech) and detected using the Pierce ECL System (Cat#32106, Thermo Scientific).

Echocardiography

Transthoracic echocardiography was performed on anesthetized mice using a Visual Sonics Vevo770 Imaging System with a 30-MHz high-frequency transducer. Heart rate and left ventricular (LV) dimensions, including diastolic and systolic wall thickness and LV end-diastolic and end-systolic chamber dimensions, were measured from 2D short-axis under M-mode tracings at the level of the papillary muscle. LV mass and functional parameters, including the percentage of fractional shortening (FS) and left ventricular volume, were calculated using the above-mentioned primary

measurements and the accompanying software.

Transmission electron microscopy

Samples of myocardium (1 mm×2 mm×2 mm) were quickly removed from the left ventricle and immediately fixed in 3% phosphate-glutaraldehyde. The Electron Microscopy Core Facility of Zhejiang University post-fixed, embedded, cut, and mounted the samples. The samples were viewed using a Tecnai 10 (100 kv) transmission electron microscope (FEI). The extent of ultrastructural damage was quantified using the Flameng score(13). For each sample, five fields of view were randomly selected, and 20 mitochondria were examined in each field of view.

Mitochondrial function assays

Mitochondria-enriched fractions were isolated from the fresh hearts of mice using the mitochondrial isolation kit (MITOISO1, Sigma-Aldrich). The ATP level was examined in platelet lysates using an ATP Assay Kit (Beyotime) in accordance with the manufacturer's instructions.

Analysis of mitochondrial membrane potential (ΔΨm)

ΔΨm was measured using the sensitive fluorescent probe JC-1**,** a cationic dye of 5,5′,6,6′-tetrachloro1,1′,3,3′-tetraethyl benzimidazol carbocyanine iodide (T3168, Invitrogen). Briefly, stained mouse frozen heart slides with 2.5 mg/mL JC-1 (100 μl) at room temperature for 20 min in a darkness place. The stained slides were washed three times with PBS and then analyzed immediately with the LSM-710 confocal microscope (Zeiss). For each slide, 4 different fields were selected randomly to acquire images and the average intensity of red and green fluorescence was determined.

LC/MS analysis of phospholipids

Lipids were extracted by using the Folch procedure(14). PLs was analyzed using a high-performance liquid chromatograph (Dionex Ultimate 3000) equipped with a high resolution mass spectrometer (SCIEX TripleTOF 5600). Phospholipids were separated on a ACQUITY UPLC CSH C18 reversed phase column (2.1mm ×100 mm, 1.7 μm (Waters)) at a flow rate of 0.2 ml/min. The column was maintained at 40℃. The analysis was performed using gradient solvents (A and B) containing 5 mM ammonium acetate. Solvent A contained methanol: acetonitrile: water (1:1:1, v/v/v) and solvent B contained propanol: water (4:1, v/v). All solvents were LC/MS grade. The column was eluted for 0-14 min with a linear gradient from 40 % to 100 % B; 14-18 min held at100 % B; 18-18.1 min with a linear gradient from 100 % to 40 % B followed by an equilibration from 18.1 to 22 min at 40% B. Analysis was performed both in positive and negative ion mode at a resolution of 3,000 for the full MS scan in an information-dependent acquisition (IDA) mode. The scan range for MS analysis was m/z50-1200 with a accumulation time of 250 ms in the TOF MS type and 100 ms in product ion type. Ion spray voltage was set at 5.5 kV in positive mode and 4.5kV in negtive mode, and source temperature was 600℃. Ion source gas 1 and 2 were both

set at 60 psi, and curtain gas was set at 35 psi. In the product ion mode, the collision energy was set at 35 V, while the collision energy spread was set at 15 V. Analysis of LC/MS data was performed using software package Lipidview 1.3 & Peakview 2.1 & MultiQuant 3.0 (SCIEX) with an in-house generated analysis workflow and oxidized phospholipid database. Briefly, peaks with S/N ratio of more than 3 were identified and searched against oxidized phospholipid database. The species assignments were done based on three criteria: exact mass, fragmentation pattern and retention time. Values for m/z were matched within 5 ppm to identify the lipid species. The structure of identified lipids was confirmed by fragmentation analysis. The retention time of each lipid class was determined based on the retention time of the exogenously added internal standard (±2 min).

Statistical Analysis

Data were analyzed and graphed using GraphPad Prism software, and all summary data are presented as mean±s.e.m. Groups were compared using the Student's *t*<test or one-way ANOVA with Tukey's post hoc test, where appropriate. For the Kaplan-Meier survival plots, statistical significance was measured using the log-rank (Mantel-Cox) test. No blinding or randomization was performed. Differences with a *p*-value <0.05 were considered significant.

References

1. He S, *et al.* (2009) Receptor interacting protein kinase-3 determines cellular necrotic response to TNF-alpha. *Cell* 137(6):1100-1111.
2. Zhang T, *et al.* (2016) CaMKII is a RIP3 substrate mediating ischemia- and oxidative stress-induced myocardial necroptosis. *Nat Med* 22(2):175-182.
3. Zhang X, *et al.* (2016) MLKL and FADD Are Critical for Suppressing Progressive Lymphoproliferative Disease and Activating the NLRP3 Inflammasome. *Cell Rep* 16(12):3247-3259.
4. Itoh K, *et al.* (1997) An Nrf2/small Maf heterodimer mediates the induction of phase II detoxifying enzyme genes through antioxidant response elements. *Biochem Biophys Res Commun* 236(2):313-322.
5. Lipshultz SE, *et al.* (1995) Female sex and drug dose as risk factors for late cardiotoxic effects of doxorubicin therapy for childhood cancer. *N Engl J Med* 332(26):1738-1743.
6. Huang CJ, Tu CT, Hsiao CD, Hsieh FJ, & Tsai HJ (2003) Germ-line transmission of a myocardium-specific GFP transgene reveals critical regulatory elements in the cardiac myosin light chain 2 promoter of zebrafish. *Dev Dyn* 228(1):30-40.
7. Kimmel CB, Ballard WW, Kimmel SR, Ullmann B, & Schilling TF (1995) Stages of embryonic development of the zebrafish. *Dev Dyn* 203(3):253-310.
8. Zhang Z, *et al.* (2011) Ferroportin1 deficiency in mouse macrophages impairs iron homeostasis and inflammatory responses. *Blood* 118(7):1912-1922.
9. Zhang F, *et al.* (2012) Metalloreductase Steap3 coordinates the regulation of iron homeostasis and inflammatory responses. *Haematologica* 97(12):1826-1835.
10. Pamplona A, *et al.* (2007) Heme oxygenase-1 and carbon monoxide suppress the pathogenesis of experimental cerebral malaria. *Nat Med* 13(6):703-710.
11. Xin Y, *et al.* (2017) Manganese transporter Slc39a14 deficiency revealed its key role in maintaining manganese homeostasis in mice. *Cell Discov* 3:17025.
12. Donovan A, *et al.* (2005) The iron exporter ferroportin/Slc40a1 is essential for iron homeostasis. *Cell Metab* 1(3):191-200.
13. Flameng W, Borgers M, Daenen W, & Stalpaert G (1980) Ultrastructural and cytochemical correlates of myocardial protection by cardiac hypothermia in man. *J Thorac Cardiovasc Surg* 79(3):413-424.
14. Folch J, Lees M, & Sloane Stanley GH (1957) A simple method for the isolation and purification of total lipides from animal tissues. *J Biol Chem* 226(1):497-509.

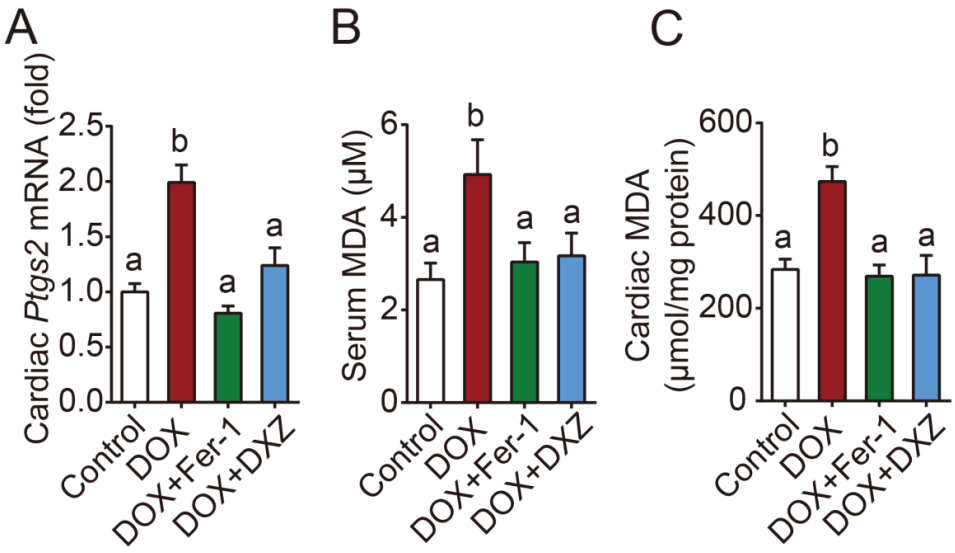

Fig. S1. Inhibiting lipid peroxidation and ferroptosis by Fer-1 and DXZ.
(A-C) Cardiac Ptgs2 mRNA (A), serum MDA (B), and cardiac MDA (C) were measured in control mice and mice treated with DOX with or without Fer-1 or DXZ (n=6 mice per group). Summary data are presented as the mean ± s.e.m. Significance was calculated using a one-way ANOVA with Tukey's post hoc-test; groups labeled with different letters differed significantly (P<0.05).

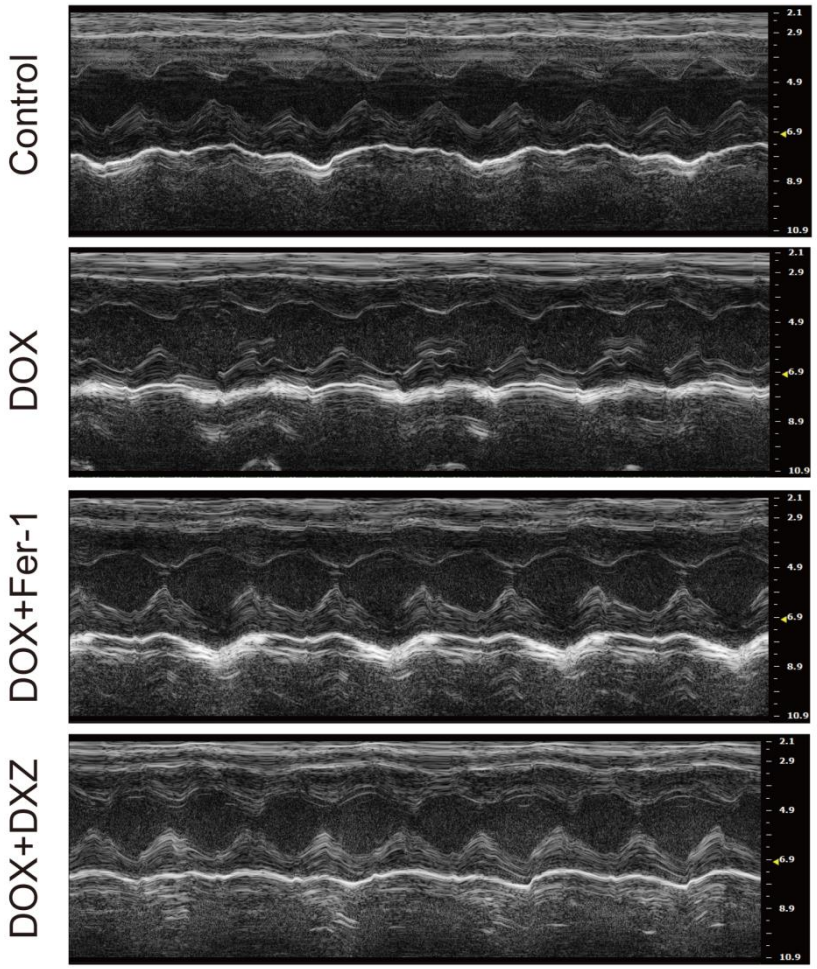

Fig. S2. Representative echocardiograms from mice subjected to DOX with Fer-1 or DXZ.

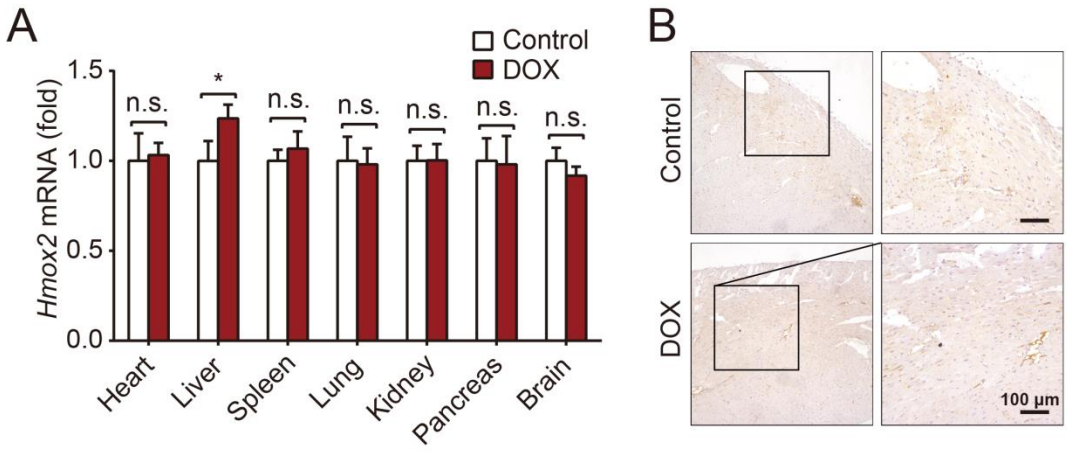

Fig. S3. The effect of DOX on Hmox2 expression.

(A) Relative levels of *Hmox2* mRNA were measured in the indicated organs on day 4 after saline or DOX treatment; n=6 for per group. (B) Representative images of Hmox2-stained heart sections from control-treated mice and mice treated with DOX. Summary data are presented as the mean ± s.e.m. Significance was calculated using the Student's *t*-test; **P*<0.05.

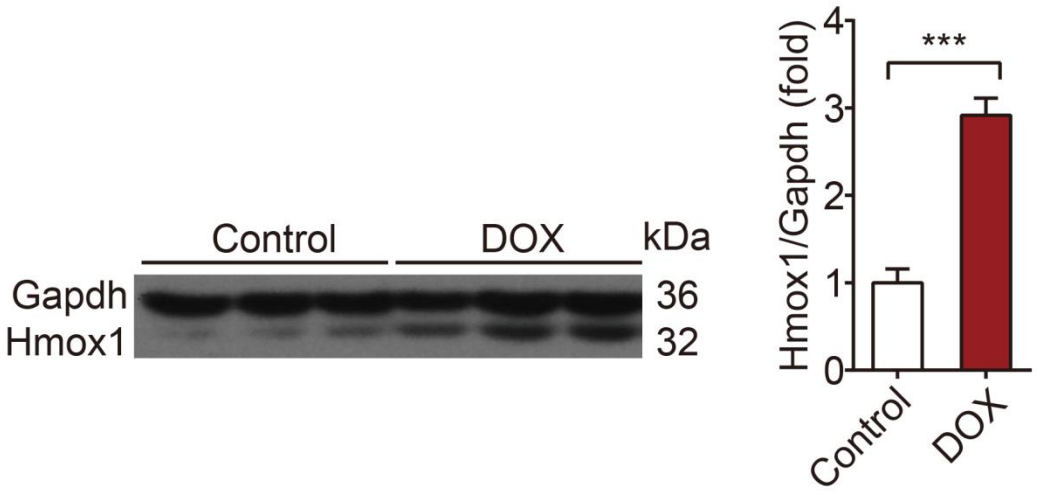

Fig. S4. Western blot (left) and quantitative analyses (right) of cardiac Hmox1 protein in control and DOX-treated mice. Gapdh was included as a loading control.

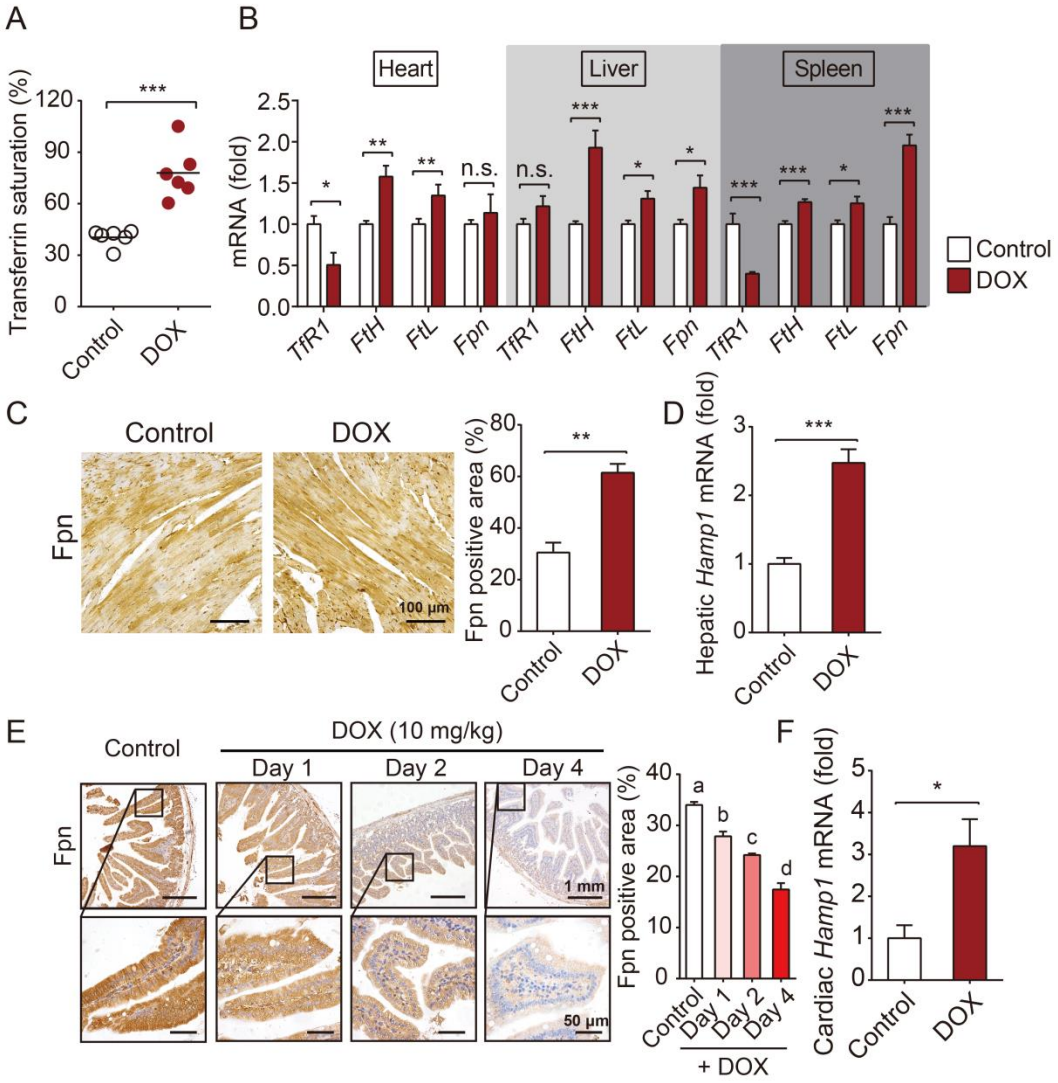

Fig. S5. DOX treatment induces rapid and systemic iron overload independent of the hepcidin-ferroportin regulatory axis.

(A) Serum transferrin saturation levels were measured on day 4 after saline or DOX treatment; n=6 mice/group. (B) Relative levels of cardiac *TfR1*, *FtH*, *FtL*, and *Fpn* mRNA were measured on day 4 after saline or DOX treatment; n=6 mice per group. (C) Representative images (left) and quantitative analyses (right) of Fpn-stained heart sections from control-treated mice and mice treated with DOX. Scale bars are indicated. (D) Relative levels of hepatic *Hamp1* mRNA were measured 4 days after control or DOX treatment; n=6 mice per group. (E) Representative images of Fpn-stained heart sections from DOX-treated and control mice; the results are summarized at the right. (F) Relative levels of cardiac *Hamp1* mRNA were measured 4 days after control or DOX treatment; n=6 for per group. Summary data are presented as the mean ± s.e.m. Significance was calculated using the Student's *t*-test; **P*<0.05; ***P*<0.01; ****P*<0.001.

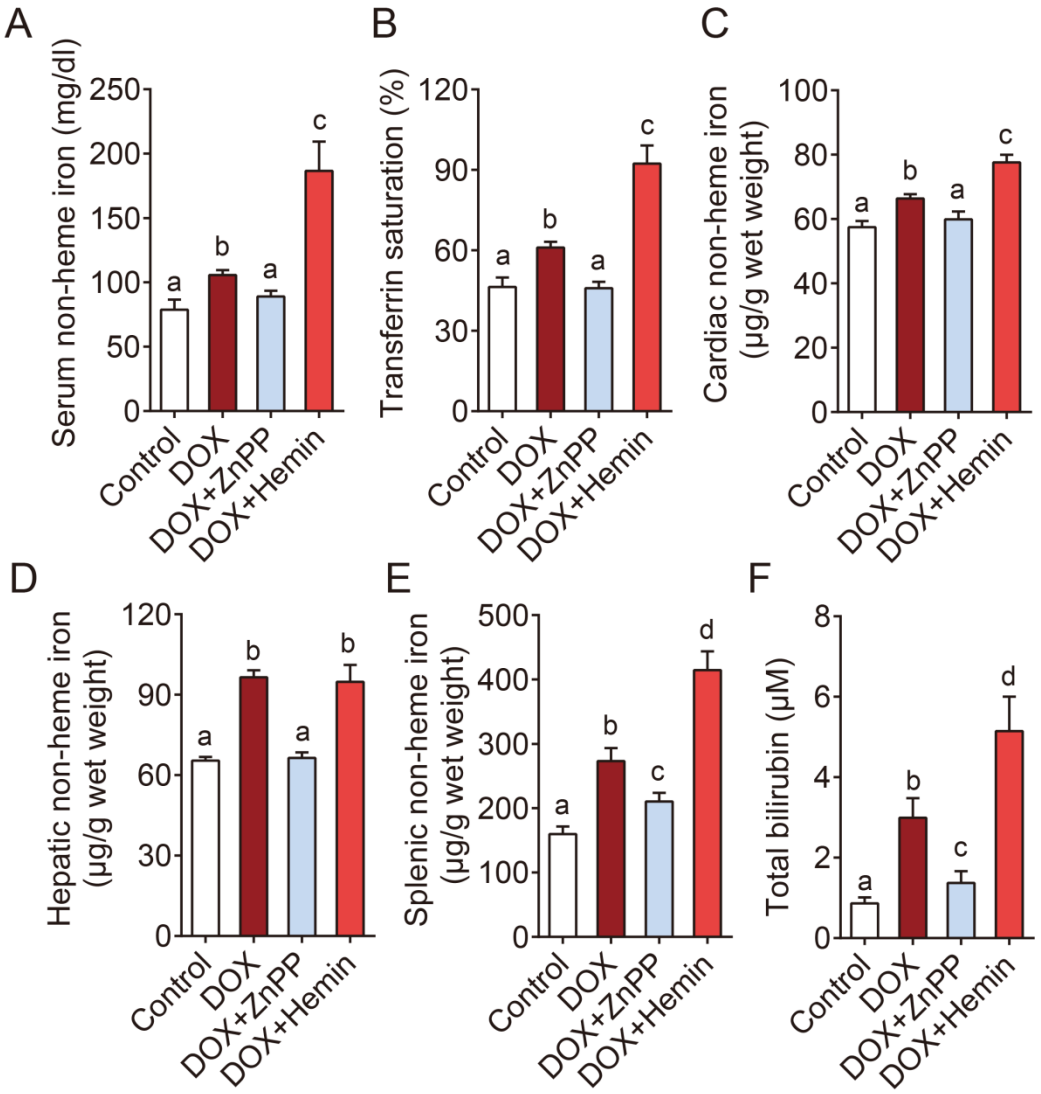

Fig. S6. The effect of ZnPP and hemin on DOX-induced iron overload in serum, liver, and spleen.

(A-B) Serum non-heme iron (A) and transferrin saturation (B) levels were measured in control-treated mice and mice treated with DOX with or without ZnPP or Hemin (n=6-7 mice per group). (C-E) Non-heme iron levels in the heart (C), liver (D), and spleen (E) were measured in control-treated mice and mice treated with DOX with or without ZnPP or Hemin (n=6-7 mice per group). (F) Serum levels of total bilirubin were measured in control-treated mice and mice treated with DOX with or without ZnPP or Hemin (n=6-7 mice per group). Summary data are presented as the mean ± s.e.m. Significance was calculated using a one-way ANOVA with Tukey's post hoc-test; groups labeled with different letters differed significantly ($P<0.05$).

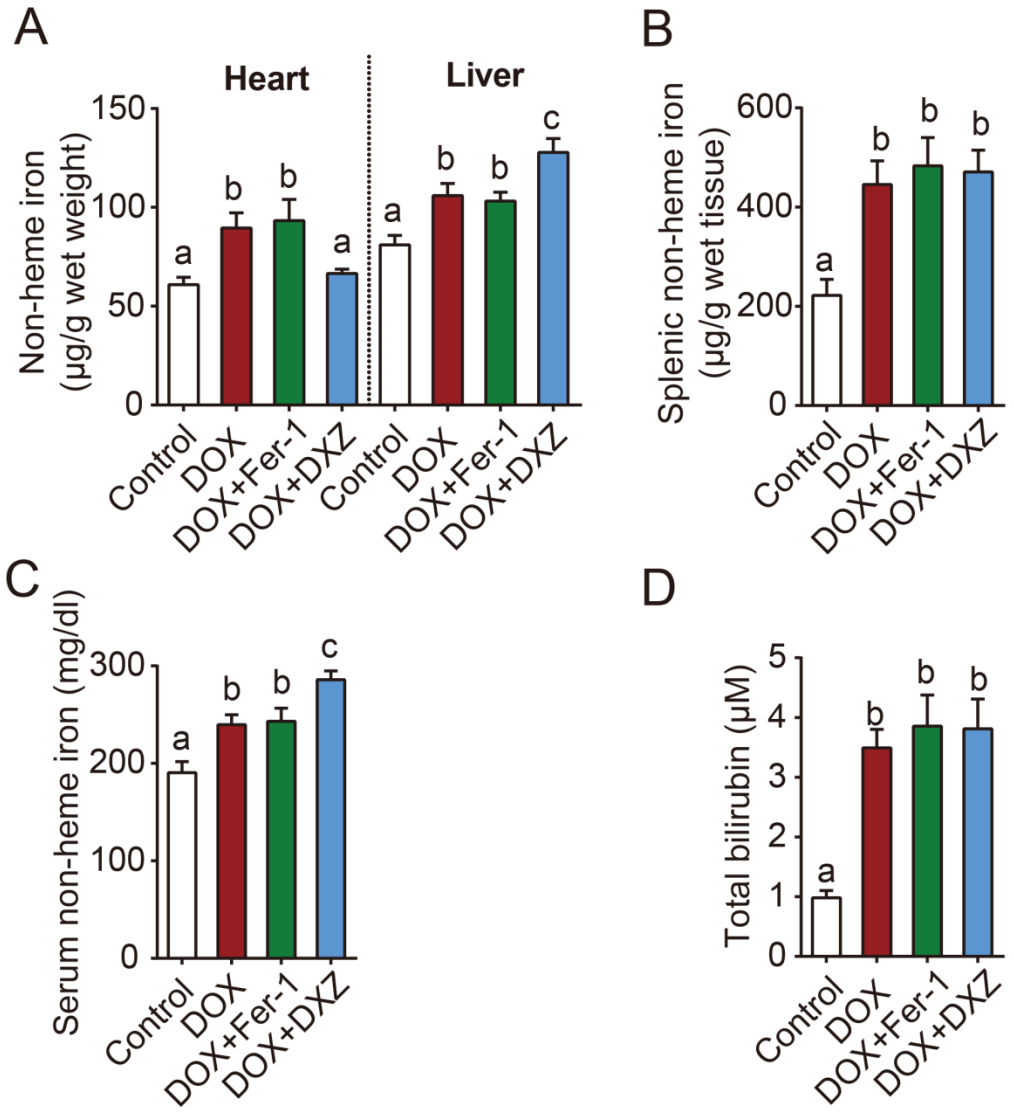

Fig. S7. Effect of Fer-1 and DXZ on DOX-induced changes in body iron status.
(A) Cardiac and hepatic non-heme iron levels were measured in control mice and mice treated with DOX with or without Fer-1 or DXZ; n=6 mice per group. (B) Serum non-heme iron levels were measured in mice treated with DOX with or without Fer-1 or DXZ. n=6 mice per group. (C) Splenic non-heme iron levels were measured in mice treated with DOX with or without Fer-1 or DXZ. n=6 mice per group. (D) Serum levels of total bilirubin were measured in mice treated with DOX with or without Fer-1 or DXZ. n=6 mice per group. Summary data are presented as the mean ± s.e.m. Significance was calculated using a one-way ANOVA with Tukey's post hoc-test; groups labeled with unlike letters were significantly different (P<0.05).

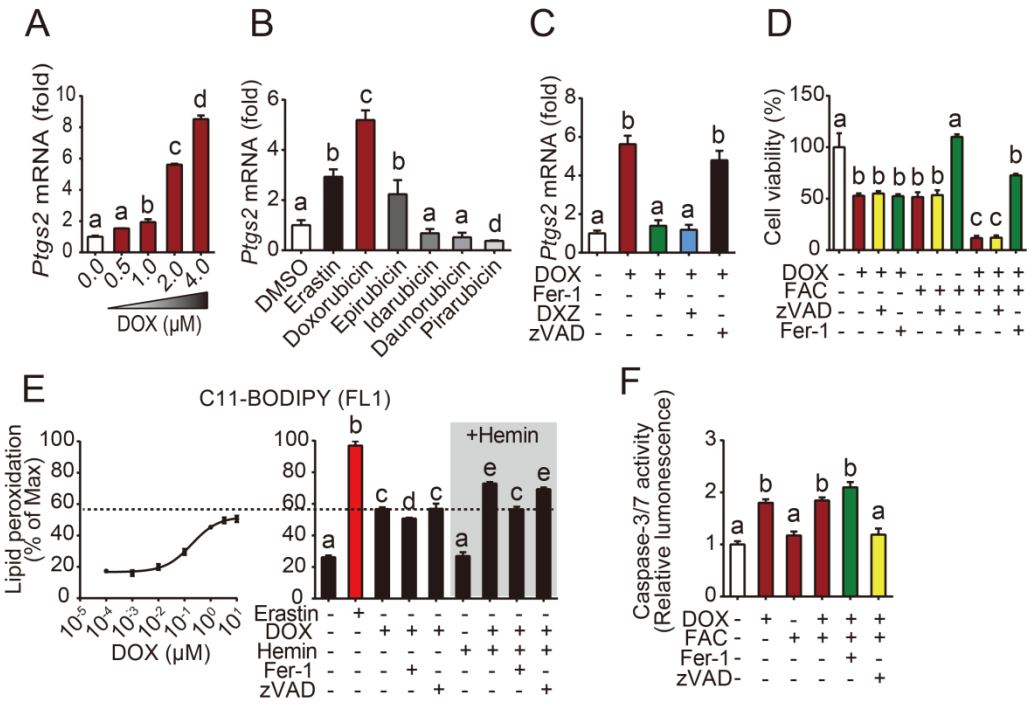

Fig. S8. DOX triggers limited lipid peroxidation *in vitro*.
(A) Relative levels of *Ptgs2* mRNA were measured in H9c2 rat cardiomyocytes after 12 h treatment with the indicated concentrations of DOX. (B) Relative levels of *Ptgs2* mRNA were measured in H9c2 rat cells after 12 h treatment with DMSO (as a control) or the indicated DOX. The ferroptosis activator erastin was used as a positive control. (C) Relative levels of *Ptgs2* mRNA were measured in H9c2 rat cardiomyocytes treated for 12 hours with or without DOX (2 μM) in the presence or absence of Fer-1 (10 μM), DXZ (100 μM), or zVAD (20 μM). (D) Cell viability was measured in H9c2 rat cardiomyocytes treated for 72 hours with or without DOX (0.1 μM) or FAC (1 mM) in the presence or absence of zVAD (1μM) or Fer-1 (2 μM). (E) (Left) Lipid peroxidation levels were measured in H9c2 rat cardiomyocytes treated with the indicated concentrations of DOX for 12 h, and lipid peroxidation was measured using flow cytometry with the fluorescent probe C11-BODIPY. (Right) H9c2 cells were control-treated or treated with DOX (2 μM), hemin (5 μM), Fer-1 (10 μM), and/or zVAD (10 μM). Erastin (2 μM) was used as a positive control. (F) Caspase 3/7 activity was measured in H9c2 rat cardiomyocytes treated for 24 hours with or without DOX (1 μM) or FAC (1 mM) in the presence or absence of Fer-1 (2 μM) or zVAD (2 μM). Summary data are presented as the mean ± s.e.m. Significance was calculated using a one-way ANOVA with Tukey's post hoc-test; groups labeled with unlike letters were significantly different (P<0.05).

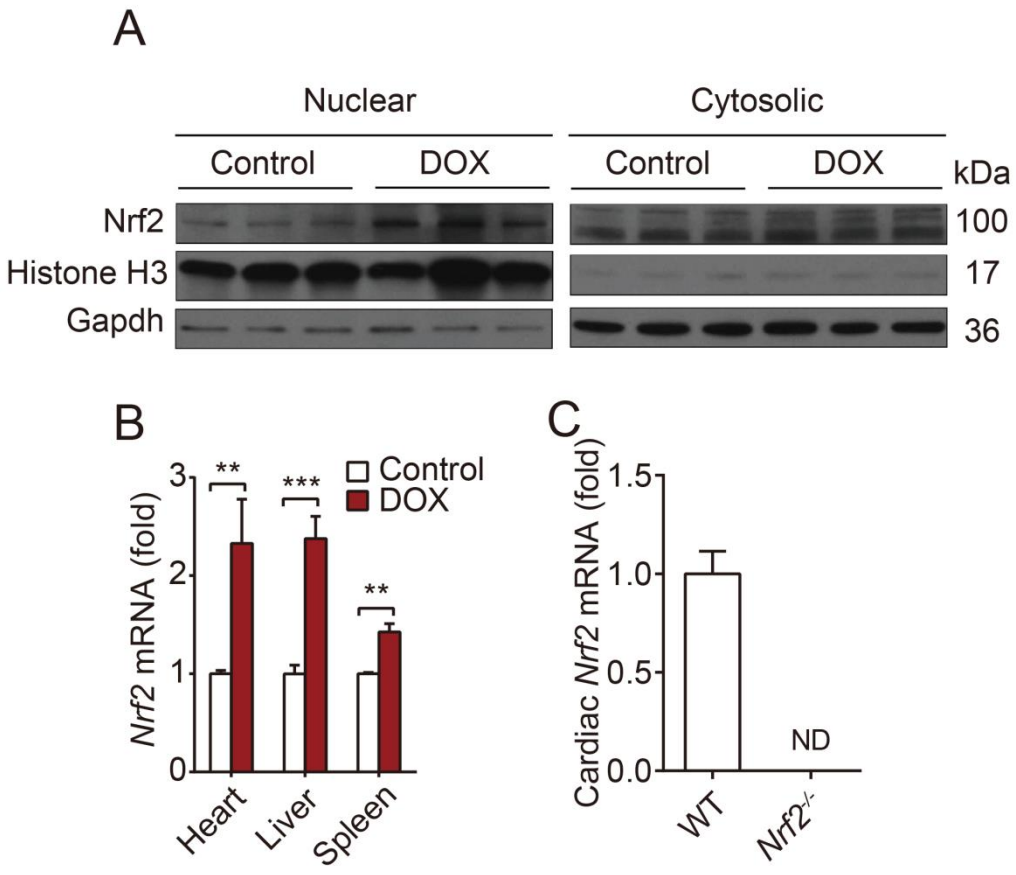

Fig. S9. The role of the transcription factor Nrf2 on DOX-induced changes in Hmox1 expression and iron metabolism.

(A) Western blot analysis of cardiac Nrf2 protein in nuclear and cytosolic fractions from control-treated and DOX-treated mice. Histone H3 and Gapdh were used as loading controls for the nuclear and cytosolic fractions, respectively. (B) Relative levels of *Nrf2* mRNA were measured in the heart, liver, and spleen of control-treated and DOX-treated mice; n=5-6 mice per group. (C) Relative levels of cardiac *Nrf2* mRNA were measured in *Nrf2*$^{-/-}$ mice and wild-type (WT) littermates; n=4-6 mice per group. Note that *Nrf2* mRNA was not detectable in the *Nrf2*$^{-/-}$ mice (ND). Summary data are presented as the mean ± s.e.m. Significance was calculated using the Student's *t*-test; **P*<0.05; ***P*<0.01.

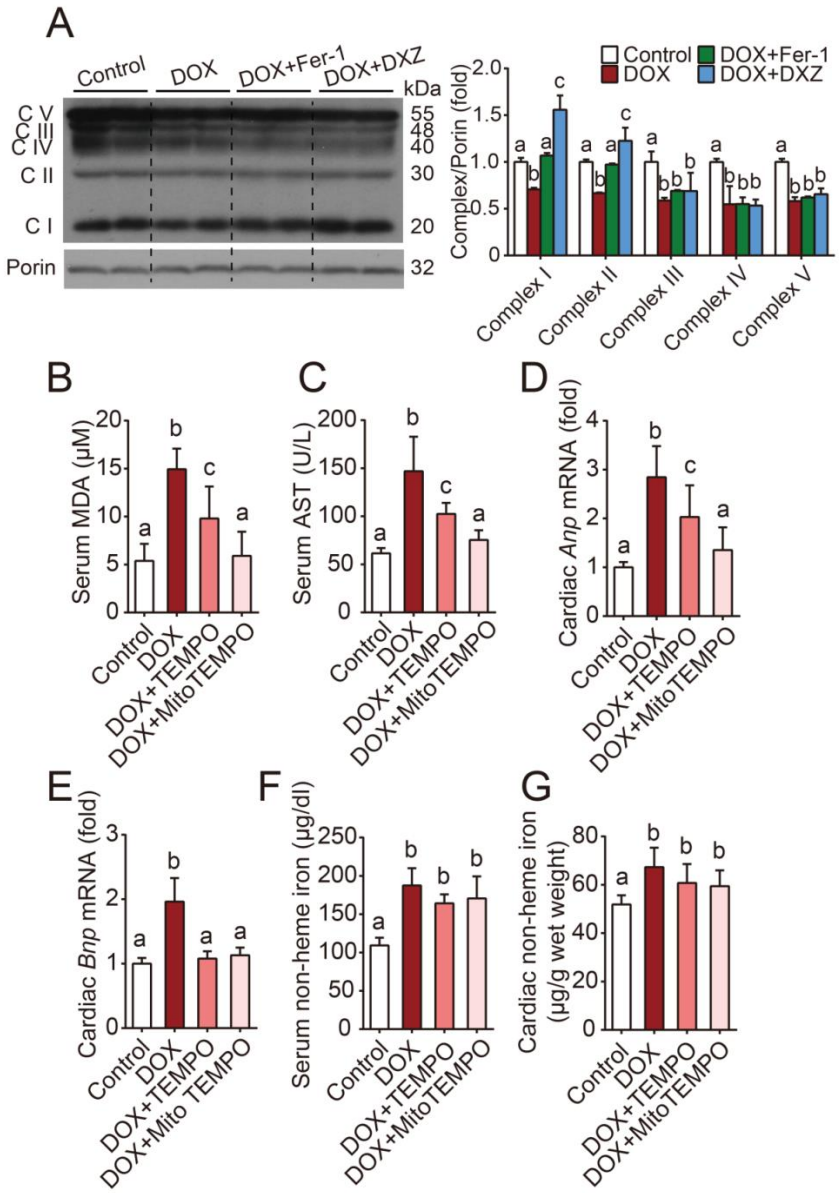

Fig. S10. The effect of MitoTEMPO and TEMPO on DOX-induced changes in cardiac function, body iron status and lipid peroxidation.

(A) Western blot analysis of OXPHOS complexes I-V (CI-CV) in mitochondria from hearts of mice subjected to DOX with or without Fer-1 or DXZ (left); and quantification of complexes (right). (B) Serum levels of aspartate transaminase (AST) were measured in mice treated with DOX with or without TEMPO or MitoTEMPO. n=6 mice per group. (C, D) Relative cardiac mRNA levels of the cardiac hypertrophy biomarkers *Anp* (C) and *Bnp* (D) in mice treated with DOX with or without TEMPO or MitoTEMPO; n=6 mice per group. (E-G) Serum non-heme iron levels (E), cardiac non-heme iron levels (F), and serum MDA levels (G) were measured in mice treated with DOX with or without TEMPO or MitoTEMPO. n=6 mice per group. Summary data are presented as the mean ± s.e.m. Significance was calculated using a one-way ANOVA with Tukey's post hoc-test; groups labeled with unlike letters were significantly different ($P<0.05$).

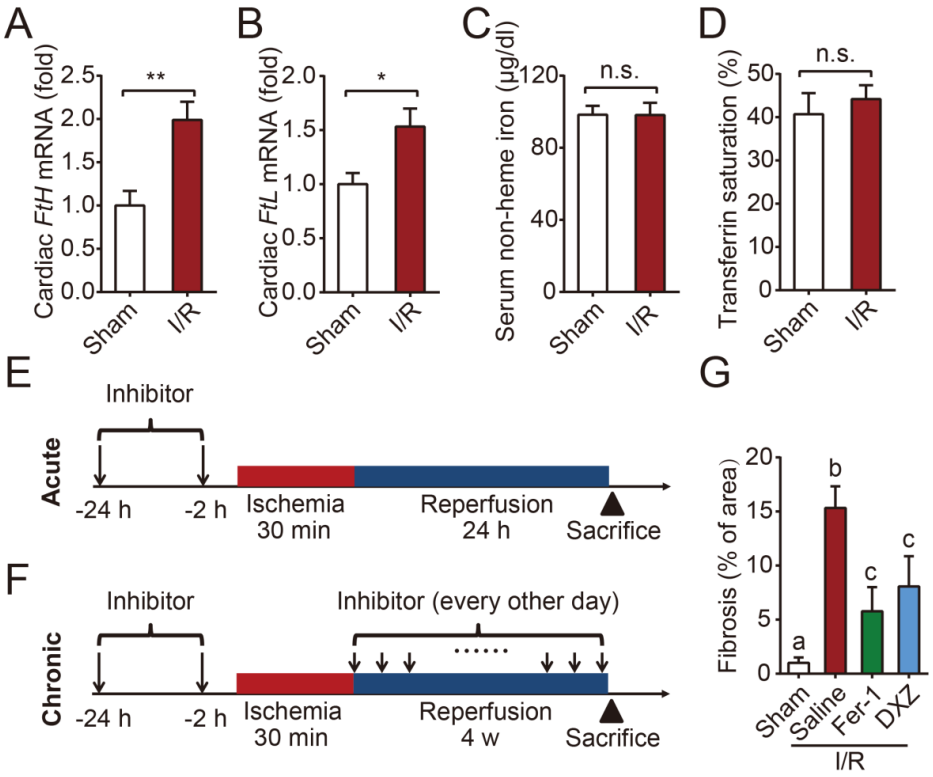

Fig. S11. The effect of Fer-1 and DXZ on iron metabolism and cardiac functions in a murine myocardial I/R injury model.

(A, B) Relative cardiac mRNA levels of *FtH* (A) and *FtL* (B) were measured in the mice subjected to sham or 30min/24h I/R injury. n=6-8 mice per group. (C, D) Serum non-heme iron (C) and transferrin saturation (D) were measured in mice subjected to sham or 30min/24h I/R injury. n=6-8 mice per group. (E, F) Acute (E) and chronic (F) *in vivo* I/R in mouse hearts (30-min ischemia followed by 24-h or 4-week reperfusion, respectively). (G) Quantitative fibrosis (% of area) measured by Masson's trichrome staining of heart sections from mice subjected to sham and 30min/4wk I/R injury with saline, Fer-1 or DXZ. Summary data are presented as the mean ± s.e.m. Significance in A-D was calculated using the Student's *t*-test; **P*<0.05; ***P*<0.01. Significance in G was calculated using a one-way ANOVA with Tukey's post hoc-test; groups labeled with unlike letters were significantly different (*P*<0.05).

Table S1. List of genes that were significantly upregulated/ downregulated based on RNA-seq analysis

Gene	ID	Fold change	*P*-value
Up-regulated			
Cdkn1a	ENSMUSG00000023067	4.859180144	2.53E-57
Hmox1	ENSMUSG00000005413	4.734363854	3.54E-50
Aox1	ENSMUSG00000063558	2.969652193	2.20E-39
Ifit1	ENSMUSG00000034459	3.768316472	4.12E-33
Rnf213	ENSMUSG00000070327	2.537918869	3.30E-31
Gm45836	ENSMUSG00000110631	4.136685644	3.77E-31
Mt1	ENSMUSG00000031765	2.254439749	9.61E-29
Irf7	ENSMUSG00000025498	2.878341821	4.36E-28
Gclm	ENSMUSG00000028124	2.494582871	5.95E-27
Gbp6	ENSMUSG00000104713	3.218097143	1.01E-25
Hist1h1c	ENSMUSG00000036181	2.23435256	7.37E-25
Oas2	ENSMUSG00000032690	3.08904087	4.49E-24
Ctnnal1	ENSMUSG00000038816	2.618383865	5.75E-24
Serpina3n	ENSMUSG00000021091	3.526119728	2.14E-23
Iigp1	ENSMUSG00000054072	2.087823094	3.50E-22
Myh7	ENSMUSG00000053093	2.168279184	1.08E-19
Ifi44	ENSMUSG00000028037	3.937600417	2.39E-19
Ifit3	ENSMUSG00000074896	3.056514346	1.18E-16
Oasl2	ENSMUSG00000029561	2.822208516	6.36E-16
Ifi213	ENSMUSG00000073491	4.692323618	6.56E-16
Cngb3	ENSMUSG00000056494	2.414015256	6.62E-16
Stat2	ENSMUSG00000040033	2.169612504	3.28E-15
Zbp1	ENSMUSG00000027514	3.743347834	1.28E-14
Gbp4	ENSMUSG00000079363	2.222808411	1.73E-14
Ifi204	ENSMUSG00000073489	2.390389708	5.56E-14
Gbp10	ENSMUSG00000105096	7.046855345	6.75E-14
Spock2	ENSMUSG00000058297	2.197364127	1.58E-12
Gm10032	ENSMUSG00000057913	5.187863973	2.48E-12
Isg15	ENSMUSG00000035692	2.753656659	1.48E-11
Rtp4	ENSMUSG00000033355	2.324413175	4.61E-11
C4b	ENSMUSG00000073418	2.081344248	7.06E-11
Tgtp1	ENSMUSG00000078922	2.681436708	7.52E-11
Phf11d	ENSMUSG00000068245	2.089513463	8.91E-11
Siglec1	ENSMUSG00000027322	2.482093153	1.08E-10
Trim30a	ENSMUSG00000030921	2.01308772	3.13E-10
Acsm5	ENSMUSG00000030972	2.29153805	3.59E-10
Trim30d	ENSMUSG00000057596	2.793471371	3.75E-10
Slfn1	ENSMUSG00000078763	6.907164168	5.66E-10
Ifi27l2a	ENSMUSG00000079017	2.085122947	1.07E-09
Oas1a	ENSMUSG00000052776	2.646998807	2.18E-09

Ifi209	ENSMUSG00000043263	3.340508572	2.85E-09
Cnksr1	ENSMUSG00000028841	2.15002196	5.83E-09
Apod	ENSMUSG00000022548	2.697316803	0.000000017
Tgtp2	ENSMUSG00000078921	2.418307226	1.73E-08
Dhx58	ENSMUSG00000017830	3.142695583	1.97E-08
Ano5	ENSMUSG00000055489	3.911473	2.87E-08
Ifit3b	ENSMUSG00000062488	2.52987347	3.28E-08
Gm4951	ENSMUSG00000073555	3.188454367	3.57E-08
Mx1	ENSMUSG00000000386	5.483118913	3.64E-08
BC023105	ENSMUSG00000063388	3.604748884	3.92E-08
Igtp	ENSMUSG00000078853	2.502329329	0.00000012
Ifi206	ENSMUSG00000037849	3.600719867	0.000000158
Slc10a6	ENSMUSG00000029321	2.206301763	0.000000179
Ddx60	ENSMUSG00000037921	2.129061154	0.000000182
Tcf23	ENSMUSG00000006642	2.448935481	0.000000183
Ifi208	ENSMUSG00000066677	3.09105525	0.000000216
Eda2r	ENSMUSG00000034457	2.358264265	0.000000273
Ifi47	ENSMUSG00000078920	2.575719512	0.000000278
Oas1b	ENSMUSG00000029605	2.977469295	0.000000372
Gm4841	ENSMUSG00000068606	5.20352729	0.000000497
S100a9	ENSMUSG00000056071	9.441132669	0.000000659
Tnip3	ENSMUSG00000044162	2.46204836	0.000000693
Gm10138	ENSMUSG00000100954	2.988909642	0.000000852
Oas1g	ENSMUSG00000066861	3.938743304	0.000000862
Slfn8	ENSMUSG00000035208	2.618331585	0.00000121
Gm45805	ENSMUSG00000110626	2.944560537	0.00000135
Nlrc5	ENSMUSG00000074151	2.16063103	0.00000152
Cxcl13	ENSMUSG00000023078	2.876302041	0.00000155
Oasl1	ENSMUSG00000041827	2.891209417	0.00000232
4933431K23Rik	ENSMUSG00000086451	2.04860873	0.00000379
Trim34a	ENSMUSG00000056144	2.042586972	0.00000449
Gvin1	ENSMUSG00000045868	2.031547627	0.00000487
Ccl8	ENSMUSG00000009185	4.880121463	0.00000578
AC153370.2	ENSMUSG00000112478	2.715263384	0.00000687
Fstl4	ENSMUSG00000036264	3.290850012	0.000011
Mx2	ENSMUSG00000023341	2.309086847	0.0000116
Usp18	ENSMUSG00000030107	2.053031921	0.0000129
Arntl	ENSMUSG00000055116	2.994629774	0.0000166
Ddias	ENSMUSG00000030641	4.44919503	0.0000225
Slfn4	ENSMUSG00000000204	14.0782378	0.0000256
Itih4	ENSMUSG00000021922	2.718516943	0.0000302
Irgm2	ENSMUSG00000069874	2.113730961	0.0000331
Oas3	ENSMUSG00000032661	3.864972729	0.0000382
Retn	ENSMUSG00000012705	2.798505396	0.0000674

Cxcr2	ENSMUSG00000026180	10.42878299	0.0000681
Gm11827	ENSMUSG00000086765	3.479522375	0.0000812
Gm45018	ENSMUSG00000108626	3.512260632	0.0000815
Clec18a	ENSMUSG00000033633	3.063378458	0.0000885
Ankrd45	ENSMUSG00000044835	2.167500952	0.00011825
Gm42923	ENSMUSG00000105134	2.015308805	0.000138168
2900052L18Rik	ENSMUSG00000043993	2.148833564	0.000195215
2900052N01Rik	ENSMUSG00000099696	7.774981717	0.000202381
Igsf23	ENSMUSG00000040498	2.001127998	0.000204873
Gm15328	ENSMUSG00000086095	2.485302171	0.000215372
Rasl10a	ENSMUSG00000034209	2.007833753	0.000334123
Cacng6	ENSMUSG00000078815	2.214625608	0.000357855
5930430L01Rik	ENSMUSG00000106951	2.205600337	0.000370355
Lrrc52	ENSMUSG00000040485	2.389173675	0.00037277
Fam124b	ENSMUSG00000043230	4.19645056	0.00044277
Gm12185	ENSMUSG00000048852	3.168699618	0.000628343
Slc9a4	ENSMUSG00000026065	4.817651553	0.000680667
Gabrr2	ENSMUSG00000023267	2.13794698	0.001008019
Hist1h1e	ENSMUSG00000051627	2.484020348	0.001031478
Klk1b26	ENSMUSG00000053719	7.735072617	0.001142131
Acaa1b	ENSMUSG00000010651	3.769316296	0.001186629
Down-regulated			
Tfrc	ENSMUSG00000022797	0.170595558	1.15E-72
Tuba4a	ENSMUSG00000026202	0.243769371	1.96E-52
Lrrc15	ENSMUSG00000052316	0.407415359	3.40E-20
Nrep	ENSMUSG00000042834	0.408697549	5.40E-20
Alas1	ENSMUSG00000032786	0.4298554	1.26E-18
Hba-a2	ENSMUSG00000069917	0.372347828	1.28E-18
Alas2	ENSMUSG00000025270	0.267753545	9.30E-17
Apln	ENSMUSG00000037010	0.324009844	4.10E-16
Lrat	ENSMUSG00000028003	0.140730892	1.78E-15
Ccnd1	ENSMUSG00000070348	0.482587456	2.04E-15
Npr3	ENSMUSG00000022206	0.486489163	1.89E-14
Efnb3	ENSMUSG00000003934	0.485777836	3.92E-13
Gm28661	ENSMUSG00000102070	0.280187342	3.96E-13
Ip6k3	ENSMUSG00000024210	0.434780337	1.71E-12
Hba-a1	ENSMUSG00000069919	0.361294582	2.06E-12
Hr	ENSMUSG00000022096	0.425315093	9.29E-12
Rtn4r	ENSMUSG00000043811	0.315058651	1.73E-11
Foxo6os	ENSMUSG00000084929	0.384586643	3.11E-11
Fbxl22	ENSMUSG00000050503	0.492233062	7.42E-11
Hbb-bt	ENSMUSG00000073940	0.430095759	1.74E-10
Hbb-bs	ENSMUSG00000052305	0.397909799	4.51E-10
Col15a1	ENSMUSG00000028339	0.480954681	2.38E-09

Mdga1	ENSMUSG00000043557	0.437976265	5.02E-09
Lrrc4b	ENSMUSG00000047085	0.441165516	6.18E-09
Meox1	ENSMUSG00000001493	0.439989208	0.000000012
Egr1	ENSMUSG00000038418	0.331423142	2.04E-08
Epn3	ENSMUSG00000010080	0.491108001	2.59E-08
Itgb6	ENSMUSG00000026971	0.39848496	3.29E-08
Mki67	ENSMUSG00000031004	0.356471343	0.000000101
Ciart	ENSMUSG00000038550	0.490217507	0.000000355
Papln	ENSMUSG00000021223	0.431774858	0.000000489
Snca	ENSMUSG00000025889	0.226147171	0.000000984
Ighv1-9	ENSMUSG00000094694	NA	0.00000106
Sez6l2	ENSMUSG00000030683	0.368271941	0.00000127
Top2a	ENSMUSG00000020914	0.253198861	0.00000191
Gm28979	ENSMUSG00000101941	0.333566308	0.00000247
Aplnr	ENSMUSG00000044338	0.46059831	0.00000473
Kcnk2	ENSMUSG00000037624	0.404860779	0.000012
Lmnb2	ENSMUSG00000062075	0.490137929	0.0000209
Ackr4	ENSMUSG00000079355	0.481148376	0.0000215
Fosb	ENSMUSG00000003545	0.376484547	0.0000265
Slc4a1	ENSMUSG00000006574	0.128806359	0.0000427
Akap5	ENSMUSG00000021057	0.378414092	0.0000642
Kdelr3	ENSMUSG00000010830	0.492887621	0.0000919
Gm12002	ENSMUSG00000086584	0.49614492	0.000113741
Pigr	ENSMUSG00000026417	0.18809349	0.000254686
Cd109	ENSMUSG00000046186	0.463734911	0.00034739
Kif18b	ENSMUSG00000051378	0.048231069	0.000620655
Mycn	ENSMUSG00000037169	0.42007747	0.000817654
Comp	ENSMUSG00000031849	0.470142787	0.000925937
Snord91a	ENSMUSG00000077493	0.15757037	0.001011476

Table S2. Hematologic parameters in control mice and DOX-treated mice

	Control (n=8)	**DOX (10mg/kg) (n=8)**	***P*-value[a]**
WBC (10^9/L)	2.44 ± 0.99	1.27 ± 0.42	<0.01
RBC (10^{12}/L)	9.18 ± 0.35	9.69 ± 0.98	0.18
HGB (g/dL)	14.20 ± 0.60	13.41 ± 0.54	<0.05
HCT (%)	46.31 ± 4.69	51.59 ± 7.10	0.10
MCV (fL)	50.61 ± 6.41	53.10 ± 3.50	0.35
MCH (Pg)	15.48 ± 0.42	15.51 ± 0.25	0.83
MCHC (g/dL)	31.03 ± 4.15	29.38 ± 2.46	0.35
PLT (10^9/L)	1167.63 ± 157.79	1504.00 ± 161.14	<0.001

All data presented at the mean ± s.e.m.

[a] Student's *t*-test (unpaired, 2-tailed).

WBC, white blood cell count; RBC, red blood cell count; HGB, hemoglobin; HCT, hematocrit; MCV, mean corpuscular volume; MCH, mean corpuscular hemoglobin; MCHC, mean corpuscular hemoglobin concentration; PLT, platelet count.

Table S3. Sequences of the primers used for real-time RT-PCR analysis

Gene	Species	Forward primer (5'→3')	Reverse primer (5'→3')
Gapdh	Rat	CCGCATCTTCTTGTGCAGTG	GAGAAGGCAGCCCTGGTAAC
Gapdh	Mouse	ATCATCCCTGCATCCACT	ATCCACGACGGACACATT
Ptgs2	Rat	ATGTTCGCATTCTTTGCCCAG	TACACCTCTCCACCGATGAC
Ptgs2	Mouse	CTGCGCCTTTTCAAGGATGG	GGGGATACACCTCTCCACCA
Hmox1	Mouse	GGTGATGGCTTCCTTGTACC	AGTGAGGCCCATACCAGAAG
Hmox2	Mouse	ACCGAGCAGAAAATACCCAGT	GTTGCGGTCCATTTCCTCCTC
Anp	Mouse	TCGTCTTGGCCTTTTGGCT	TCCAGGTGGTCTAGCAGGTTCT
Bnp	Mouse	AAGTCCTAGCCAGTCTCCAGA	GAGCTGTCTCTGGGCCATTTC
Myh7	Mouse	GCTGAAAGCAGAAAGAGATTATC	TGGAGTTCTTCTCTTCTGGAG
FtH	Mouse	CCATCAACCGCCAGATCAAC	GAAACATCATCTCGGTCAAA
FtL	Mouse	CGTCTCCTCGAGTTTCAGAAC	CTCCTGGGTTTTACCCCATTC
Fpn	Mouse	GTGGAGTACTTCTTGCTCTGG	CTGCTTCAGTTCTGACTCCTC
TfR1	Mouse	CTCAGTTTCCGCCATCTCAGT	GCAGCTCTTGAGATTGTTTGCA
Mt1	Mouse	GCGTCACCACG ACTTCAAC	GTCACATCAGGCACAGCAC
Hamp1	Mouse	GCACCACCTATCTCCATCAACA	TTCTTCCCCGTGCAAAGG
Nrf2	Mouse	AGTGACTCGGAAATGGAGGAG	TGTGCTGGCTGTGCTTTAGG
mt-Atp6	Mouse	ATTAGCCCACCAACAGCTAC	GGCTTACTAGGAGGGTGAATAC
mt-Cytb	Mouse	GCCACCTTGACCCGATTCT	TTGCTAGGGCCGCGATAAT